Comparison of Serial and Quasi-Serial Industrial Robots for Isotropic Tasks

Alexandr Klimchik, Evgeni Magid, Ilya Afanasyev and Anatol Pashkevich

Abstract The paper presents a new approach for comparison of serial and quasi-serial robots in industrial applications. In contrast to other works, it is based on evaluation of maximum compliance errors in the working area for isotropic tasks. It is proved that for large-scale isotropic tasks quasi-serial manipulators with kinematic parallelograms are preferable, while for small task dimensions' serial manipulators provide better accuracy.

Keywords Industrial robot · Serial manipulator · Quasi-serial manipulator

1 Introduction

In modern industrial applications, a number of technological tasks can be treated as isotropic ones, where required end-effector motion direction is almost uniform. Examples of such tasks can be found in milling of contemporary high performance metal and composite materials that generate essential force/torques causing non-negligible compliance errors of robotic manipulator. To minimize these errors, robot manufactures propose quasi-serial architectures with kinematic parallelograms that potentially provide better rigidity. For this reason, practicing engineers face the problem of well-grounded selection between serial and quasi-serial architectures for particular applications. This paper presents a novel technique that

A. Klimchik (✉) · E. Magid · I. Afanasyev
Innopolis University, Universitetskaya 1, 420500 Innopolis, Russia
e-mail: a.klimchik@innopolis.ru

E. Magid
e-mail: e.magid@innopolis.ru

I. Afanasyev
e-mail: i.afanasyev@innopolis.ru

A. Pashkevich
Ecole des Mines de Nantes, 4 rue Alfred-Kastler, 44307 Nantes, France
e-mail: anatol.pashkevich@mines-nantes.fr

V. Parenti-Castelli and W. Schiehlen (eds.), *ROMANSY 21 - Robot Design, Dynamics and Control*, CISM International Centre for Mechanical Sciences 569,
DOI 10.1007/978-3-319-33714-2_47

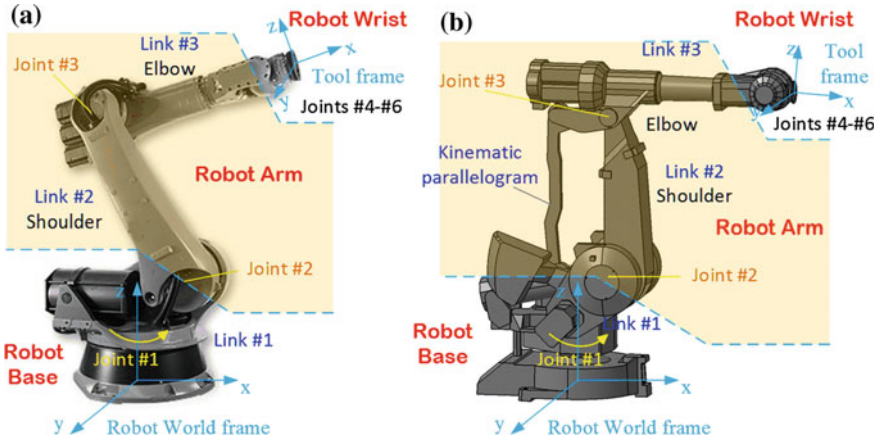

Fig. 1 Architecture of a typical industrial robot. **a** typical serial manipulator **b** typical quasi-serial manipulator

allows user to evaluate manipulator performance numerically taking into account the manipulator stiffness properties and also particularity and size of a technological task.

In general, typical *serial manipulators* contain three main components: robot base, robot arm and robot wrist (Fig. 1a), where the robot base defines the arm orientation, the robot arm is responsible for the major movements of the robot end-effector, the orientation movements are provided by the robot wrist. *Quasi-serial robots* have roughly similar architecture (see Fig. 1b). In contrast to strictly serial counterparts, a quasi-serial manipulator arm contains a kinematic parallelogram, which can be treated as an internal closed-loop (and completely differ from hybrid serial-parallel manipulators). Usually the parallelogram does not affect essentially manipulator control and does not change manipulator direct/inverse kinematic equations. On the other hand, the stiffness model of a quasi-serial manipulator essentially differs from its serial counterpart since relocation of the manipulator compliant element influences stiffness behavior. For this reason, the results obtained for strictly serial manipulators cannot be used directly for quasi-serial manipulators.

The stiffness model of a robotic manipulator describes manipulator behavior under loading (Klimchik et al. 2014; Pashkevich et al. 2011; Yan et al. 2016). In addition to the conventional robot parameters (geometric ones), it includes a number of elastic parameters describing flexibility of manipulator links and joints. In number of industrial applications, manipulator elasticity cannot be ignored since high loading is applied to the robot, while required positioning accuracy is rather high. For example, in machining application, an end-effector deflection of industrial robots under the loading of 1kN may vary from 1 to 10 mm (Matsuoka et al. 1999), while demanded accuracy for machining process is about 0.1 mm. These compliance errors can be reduced down to admissible level using both on-line and off-line

error compensation techniques that are based on the appropriate stiffness model (Klimchik et al. 2013a), which may be either "*complete*" or "*reduced*". The complete stiffness model of an industrial robot is rather complicated, as it takes into account all manipulator links and actuators compliances (Klimchik et al. 2015). However, in practice, a number of manipulator components may be treated as rigid ones, while the main compliance is concentrated in the actuator transmissions. This allows to apply so-called reduced models that take into account the joint elasticities only (Alici and Shirinzadeh 2005; Guo et al. 2015). Such models are quite common for stiffness modeling of heavy industrial robots (Klimchik et al. 2013b) where the links are massive and deflections under the force 1kN are lower than 0.1 mm. For this reason, the comparison study presented in this paper is based on the reduced stiffness model.

2 Motivation Example

To define the research problem and to demonstrate advantages/disadvantages of both serial and quasi-serial architectures, let us start with a motivation example showing that proper manipulator type selection essentially depends on the technological task dimension and external force orientation. This example deals with two manipulators (serial and quasi-serial ones) with the same basic geometric parameters $l_2 = 1\,\text{m}$, $l_3 = 0.8\,\text{m}$ and similar joint compliances $k = 10^{-6}\,\text{rad/N m}$. These values are typical for industrial robots that are used in machining (Dumas et al., 2012). To compare stiffness behavior, let us compute the compliance errors caused by an external force 1.0 kN applied to the end-effector (details of related technique are presented in (Klimchik et al. 2014)). Relevant results have been obtained for two different external loadings and are presented in Fig. 2, which shows the compliance error distribution within the workspace.

As follows from Fig. 2, the elastostatic deflections vary from 0 to 3.83 mm for the serial manipulator and from 0 to 1.62 mm for the quasi-serial manipulator. These results show that for the considered case study the compliance errors range does not depend on the force direction, however the compliance error maps differ essentially. Summarizing these results, it is possible to define several research problems that are in the focus of this paper and are useful for optimal selection of robotic manipulator from the set of available ones. These problems can be formulated as follows:

- development of the manipulator selection methodology using the compliance maps and optimal task placement technique;
- defining boundary between the technological tasks which suit serial and quasi-serial architectures in the best way.

They will be studied in the following Sections.

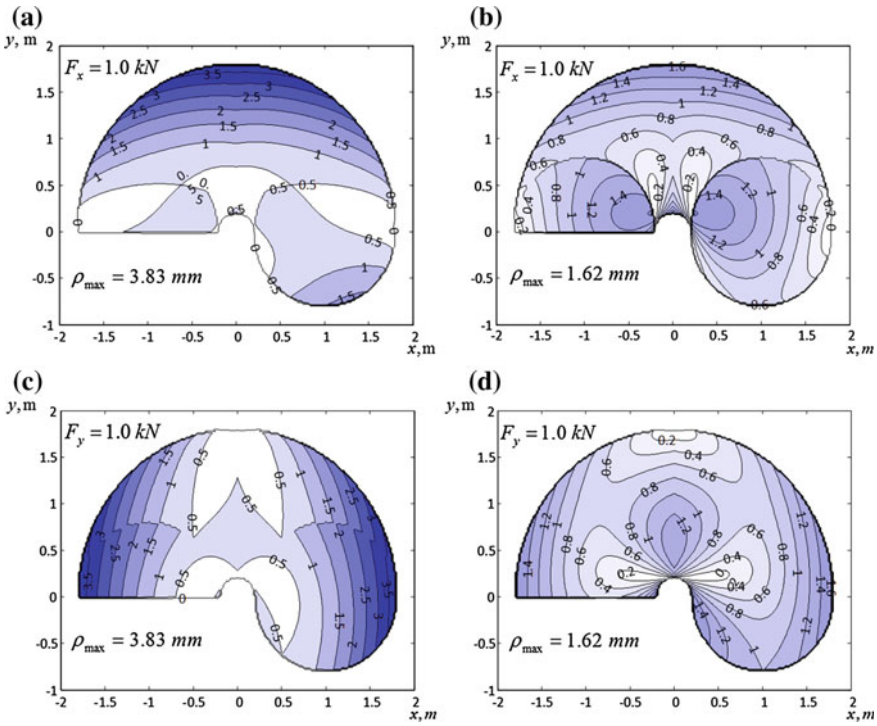

Fig. 2 Compliance maps for serial and quasi-serial manipulators. **a** Compliance map for *serial manipulator* under the external loading in x-direction **b** Compliance map for *quasi-serial manipulator* under the external loading in x-direction **c** Compliance map for *serial manipulator* under the external loading in y-direction **d** Compliance map for *quasi-serial manipulator* under the external loading in x-direction

3 Performance Measure for Manipulator Accuracy Evaluation

The manipulator performance with respect to a number of technological tasks cannot be evaluated using elastic or geometrical properties only: an appropriate performance measure should take into account also the external force/torque directions and magnitudes. The problem becomes more complicated if external loadings are not given. In this case it is reasonable to consider all possible directions of external force and to estimate maximal compliance errors in the considered work-point:

$$\rho_p = \max_{\varphi_i} |\mathbf{k}_C \cdot \mathbf{F} \cdot \mathbf{R}(\boldsymbol{\varphi}_i)|; \qquad \boldsymbol{\varphi}_i \in [-\boldsymbol{\pi}, \boldsymbol{\pi}] \tag{1}$$

where $\mathbf{k}_C = \mathbf{J}(\mathbf{q}) \cdot \mathbf{k}_\theta \cdot \mathbf{J}(\mathbf{q})^T$ is the manipulator compliance for the configuration $\mathbf{q}$, the diagonal matrix $\mathbf{k}_\theta$ collects the joint compliances, $\mathbf{F}$ is the external loading applied to the manipulator end-effector, $\mathbf{R}(\boldsymbol{\varphi}_i)$ is the rotation matrix allowing us to estimate the compliance errors for any force direction $\boldsymbol{\varphi}_i$.

In practice, the direction of maximal and minimal compliance errors can be obtained via the singular value decomposition of the compliance matrix $\mathbf{k}_C$

$$\mathbf{k}_C = \mathbf{U} \cdot \sum \cdot \mathbf{V}^T \tag{2}$$

where the diagonal matrix $\sum = diag(\sigma_{\max}, \ldots, \sigma_{\min})$ contains the singular values, $\mathbf{U}$ and $\mathbf{V}$ are orthogonal matrices that in this particular case are equal. Here, the first line of the vector $\mathbf{V}$ defines the force direction that causes the maximum compliance error of the end-effector. Similarly, the last line of vector $\mathbf{V}$ defines the strongest direction. Corresponding values of $\sigma_{\max}, \ldots, \sigma_{\min}$ define the magnitude of compliance errors and the ratio between these values allows user to compare manipulator compliance in different directions. Hence, values $\sigma_{\max}$ will be used further to estimate the manipulator stiffness properties in the configuration $\mathbf{q}$.

It is worth mentioning that manipulator architecture analysis cannot be performed in a single point. For this reason, we consider an *isotropic-shape tasks*, which can be circumscribed by a circle S of diameter d. Even though isotropic tasks may provide rather rough approximation for some complex technological problems, these it allows us to classify all technological tasks into typical groups and to analyze the manipulator performance for the group of tasks that meet certain requirements. Using the above notations, it is possible to evaluate the manipulator performance using maximum compliance error in accordance with expression

$$\rho_S = \max_{\mathbf{q}} \{\sigma_{max}(\mathbf{q}) \mid g(\mathbf{q}) \in S\} \tag{3}$$

where the function $g(\mathbf{q})$ defines the manipulator geometry, and S is a workspace area corresponding to this task. By means of this performance measure it is possible to estimate potential compliance errors caused by the tool-workpiece interaction and to compare accuracy of different manipulators for the same type of technological tasks. In fact, here the product $\rho_S \cdot |\mathbf{F}|$ corresponds to the guaranteed accuracy of robot-based machining if the cutting force does not exceed $|\mathbf{F}|$ while the workpiece is placed inside of optimally located zone S within the robot workspace.

4 Comparison of Serial and Quasi-Serial Architectures

To compare serial and quasi-serial manipulators, let us compute and evaluate the error maps within the robot workspace using Eq. (3) and varying the size and location of task workspace S. For the error maps evaluation, let us apply the optimal task placement technique that provides the best task location $\mathbf{p}_0^*$ for each given the size of d

$$[\mathbf{p}_0^*, \rho_S^*] = arg\left[\min_{\mathbf{p}_0}\max_{\mathbf{q}}\{\sigma_{max}(\mathbf{q}) \mid g(\mathbf{q}) \in S(\mathbf{p}_0, d)\}\right] \quad (4)$$

It should be noted that for both serial and quasi-serial manipulators the compliance errors do not depend on the angle q_2. It means that for the *isotropic-shape tasks* the problem of the optimal task placement reduces to a one-dimensional one with respect to q_3. Relevant algorithm allowing us to define the optimal task placement and to evaluate manipulator accuracy is presented below. It provides the benchmark task accuracy ε_S and task optimal location corresponding to the task dimension d.

Algorithm 1 – Optimal task placement for isotropic-shape tasks

Input: manipulator geometry l_1, l_2; task diameter d; stopping parameter δ
Output: optimal task location x_O; obtained accuracy ε_S
Notations: $x_{\min} = |l_1 - l_2|$, $x_{max} = l_1 + l_2$
Invoked function: error function $\varepsilon(x)$, $x \in [x_{min}, x_{max}]$; $\varepsilon(x) = Inf$ if $x \notin [x_{min}, x_{max}]$
Verify $d < x_{max} - x_{min}$, return "No Solution" if false
Find minimum of error function $[\varepsilon_{\min}, x^*] = \min(\varepsilon(x) \mid x \in [x_{min}, x_{max}])$
  Set initial values of interval $x_1 = x^*, x_2 = x^*$ and step size $d_i = d/2$
  Repeat
    Compute $\varepsilon_1 = \varepsilon(x_1 - d_i)$; $\varepsilon_2 = \varepsilon(x_2 + d_i)$
    Enlarge interval $[x_1, x_2]$:
    if $\varepsilon_1 \geq \varepsilon_2$
      than $x_2 = x_2 + d_i$
      else $x_1 = x_1 - d_i$
    Halve step size
      if $x_2 - x_1 < d - \delta$
        than $d_i = d_i / 2$
  while $x_2 - x_1 < d$
Compute task accuracy $\varepsilon_S = \max(\varepsilon(x_1), \varepsilon(x_2))$ and its location $x_O = (x_1 + x_2)/2$

Applying the above presented algorithm to the serial and quasi-serial manipulators, there were computed values of the benchmark accuracy ε_S for different task size d and different link lengths ratio $\mu = l_3/l_2$ (assuming that the total length is fixed, i.e. $l_2 + l_3 = const$, and all joint stiffness coefficients are equal). Relevant results are presented in Fig. 3, which allows us to compare potential accuracy for both architectures. As follows from them, for the *quasi-serial manipulator*, the best positioning accuracy is achieved for the link length ratio $\mu = 1.0$. It should be noted that this conclusion does not depend on the task size d. Moreover, the manipulator with such ratio may perform tasks of maximum size compared to the quasi serial manipulators with $\mu > 1.0$ and $\mu < 1.0$. In contrast, for a *serial manipulator*, the optimal link length ratio essentially depends on the task size. In particular, for small tasks with $d/(l_2 + l_3) < 0.25$ it is preferable to have the link length ratio $\mu = 0.7$

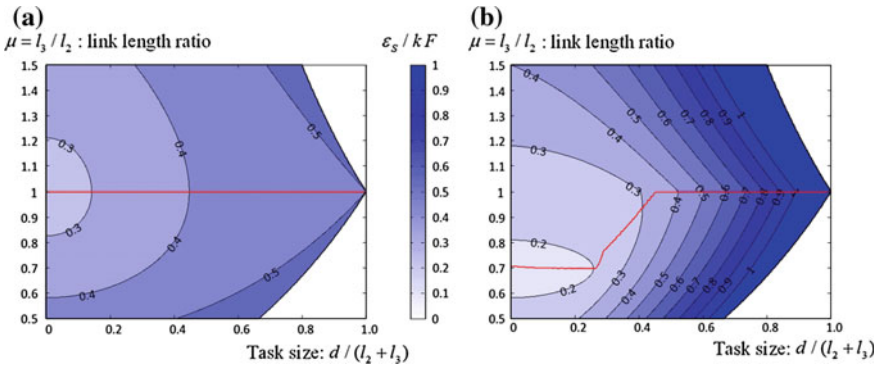

Fig. 3 Normalized accuracy ε_S / kF for isotropic tasks. **a** Case of the quasi-serial manipulator **b** Case of the serial manipulator

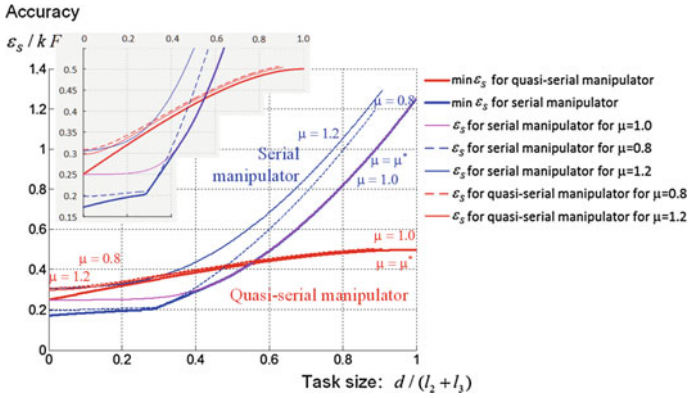

Fig. 4 Accuracy of serial and quasi-serial manipulators for isotropic task

while for large tasks with $d/(l_2 + l_3) > 0.4$ the optimal ratio is $\mu = 1.0$. For convenience, optimal values of μ are highlighted in Fig. 3 by red lines.

To make comparison of two architectures more evident, Fig. 4 presents potential accuracy (as well as zoom) for isotropic-shape tasks that is achieved for different link-length ratios μ. The latter includes the optimal value of $\mu = \mu^*$ as well as $\mu = 0.8,\ 1.0,\ 1.2$ that are widely used in practice. The results show that for small isotropic-shape tasks the serial manipulators are preferable since they are able to ensure better accuracy. On the other side, the quasi-serial manipulators are better if the task size is rather big, i.e. $d/(l_2 + l_3) > 0.55$. Besides, the quasi-serial manipulators provide similar performance for both small and large tasks while the properties of their serial counterparts essentially depend on the task size. It should be also emphasized that the link length ratio in the range $\mu \in [0.8;\ 1.2]$ does not affect essentially the accuracy of a quasi-serial manipulator. In contrast, a serial

Table 1 Accuracy of serial (SM) and quasi-serial (QSM) manipulators for isotropic tasks

		Normalized accuracy, $\varepsilon_S / k F$							
Task dimension $d/(l_2 + l_3)$		0.1		0.2		0.5		0.8	
Manipulator architecture		SM	QSM	SM	SM	SM	QSM	SM	QSM
Link-length ratio μ	0.8	*0.20*	0.32	*0.21*	0.34	0.45	0.43	1.00	0.49
	1.0	0.25	0.28	0.25	0.32	*0.37*	0.42	0.82	*0.48*
	1.2	0.31	0.31	0.33	0.34	0.55	0.43	1.05	0.49
Minimum error		*0.18*	0.28	*0.19*	0.32	*0.37*	0.42	0.82	*0.48*

manipulator is very sensitive to its proper selection; for the range $\mu \in [0.8;\ 1.2]$ the serial manipulator accuracy may be twice as worse compared to the minimum value. The results of this study are summarized in Table 1, which shows accuracy limits and preferred manipulators (for which the table cells are colored in green).

5 Conclusion

The paper presents the comparison analysis of serial and quasi-serial manipulators for isotropic-shape tasks. It proposes a new technique that evaluates robot positioning accuracy taking into account the manipulator stiffness behavior within the working area. It was demonstrated that serial manipulators are preferable for small tasks while quasi-serial manipulators better suit large tasks. Also it was shown that, from the manipulator compliance point of view, it is preferable to have serial manipulators with link-length ratio about 0.7 and quasi-serial with equal link lengths. In future, the developed approach will be applied to compare robot architectures from different manufactures.

References

Alici, G. & Shirinzadeh, B. (2005) Enhanced stiffness modeling, identification and characterization for robot manipulators. *Robotics, IEEE Tranaction. on 21*(4), 554–564.

Dumas, C., Caro, S., Cherif, M., Garnier, S., & Furet, B. (2012). Joint stiffness identification of industrial serial robots. *Robotica, 30*, 649–659.

Guo, Y., Dong, H., & Ke, Y. (2015). Stiffness-oriented posture optimization in robotic machining applications. *Robotics and Computer-Integrated Manufacturing, 35*, 69–76.

Klimchik, A., Chablat, D., & Pashkevich, A. (2014). Stiffness modeling for perfect and non-perfect parallel manipulators under internal and external loadings. *Mechanism and Machine Theory, 79*, 1–28.

Klimchik, A., Furet, B., Caro, S., & Pashkevich, A. (2015). Identification of the manipulator stiffness model parameters in industrial environment. *Mechanism and Machine Theory, 90*, 1–22.

Klimchik, A., Pashkevich, A., Chablat, D., & Hovland, G. (2013a). Compliance error compensation technique for parallel robots composed of non-perfect serial chains. *Robotics and Computer-Integrated Manufacturing, 29*(2), 385–393.

Klimchik, A., Wu, Y., Dumas, C., Caro, S., Furet, B. & Pashkevich, A. (2013b) Identification of geometrical and elastostatic parameters of heavy industrial robots. In *Robotics and Automation, 2013 IEEE International Conference on* (pp. 3707–3714).

Matsuoka, S.-I., Shimizu, K., Yamazaki, N., & Oki, Y. (1999). High-speed end milling of an articulated robot and its characteristics. *Journal of Materials Processing Technology, 95*(1–3), 83–89.

Pashkevich, A., Klimchik, A., & Chablat, D. (2011). Enhanced stiffness modeling of manipulators with passive joints. *Mechanism and Machine Theory, 46*(5), 662–679.

Yan, S. J., Ong, S. K., & Nee, A. Y. C. (2016). Stiffness analysis of parallelogram-type parallel manipulators using a strain energy method. *Robotics and Computer-Integrated Manufacturing, 37*, 13–22.